



Numerical Investigation of the Scale Effect on the Flow around the Ship by using RANSE Method

Tat-Hien Le^{1,2,*}, Tran Van Tao^{1,2}

¹ Ho Chi Minh City University of Technology (HCMUT), Vietnam

² Vietnam National University Ho Chi Minh City, Vietnam

ARTICLE INFO

Article history:

Received 27 February 2023

Received in revised form 24 March 2023

Accepted 20 April 2023

Available online 1 November 2023

Keywords:

Flow; RANSE; Scale Effect; Resistance

ABSTRACT

The paper deals with the numerical simulation results of scale effect on flow field around ship by using RANSE method. The differences in resistance coefficient components and flow around the ship such as wave pattern on free surface, wave profile along the hull of the ship, dynamic pressure and wall shear stress distributions on the surface of the ship and nominal wake field between the model and full-scale ship are provided and analysed in this paper. The obtained numerical simulation results are compared with the measured data in order to verify and validate simulation results.

1. Introduction

In designing a ship, the accurate estimation of ship resistance plays a crucial role as this parameter also be a primary input of other problems related to defining the ship propulsion system and power in order to archive the designed speed. It is no deniable that conducting towing tank test then extrapolate the result into the full-scale ship currently is the most reliable ship resistance predicting method. However, towing tank test method can only ensure the similarity of geometry and Froude number between the model scale and full-scale ship and it cannot satisfy the same value of the Reynolds number, which causes the differences in the characteristics of flow around the model scale ship and the full scale one [1-4]. As a result, it is significantly important to consider these differences in various model scales that can support in identifying the accurate characteristics of flow around the ship and solving the other problems like optimizing the ship hull, designing the propeller, etc. at the full scale.

Presently, thank the considerable development of computational resources, and numerical method, RANSE method is broadly applied to solve the hydrodynamics problems in general [5-7] and ship hydrodynamic problems in particular [4,7-23]. In comparison with the experiment, RANSE method provides relatively reliable results, saving computational time and expenditure as no physical model requires [8,10,24]. In addition, RANSE also advances in simulating the ship resistance at full

* Corresponding author.

E-mail address: hienlt@hcmut.edu.vn (Tat-Hien Le)

scale. Moreover, the post-RANSE analysis can provide all necessary information on the flow around the ship characteristics.

Various authors have carried out the research of scale effect on the flow around the ship [1,3,4,25,26]. Those research results proved that model scale definitely effects on the flow field around the ship. The magnitude of difference depends on the discrepancy in model scale. Hänninen, S. and J. Sehweighofer [25] reported that resistance coefficients, wave pattern and streamlines strongly depends on the Reynolds number. Dogrul, A *et al.*, [1] presents a study of the scale effect on the ship resistance components and form factor for two different ship hull forms by RANSE method. The conclusion of authors in [1] is that the difference in boundary layers, wave pattern and viscous pressure resistance between model scale and full scale. The magnitude of these differences depends not only on the discrepancy in scale model, but also ship hull form.

Inheriting the previous studies, this research will focus on studying the impact of scale effect on the characteristics of the flow around a KCS containership by employing RANSE method.

2. Methodology

2.1 Reynolds-Averaged Navier-Stokes Equations

The Reynolds-Averaged Navier-Stokes Equations (RANSE) are defined as follows [15]:

$$\frac{\partial(\rho\bar{u}_i)}{\partial x_i} = 0 \quad (1)$$

$$\frac{\partial(\rho\bar{u}_i)}{\partial t} + \frac{\partial}{\partial x_j}(\rho\bar{u}_i\bar{u}_j + \overline{\rho u'_i u'_j}) = -\frac{\partial\bar{p}}{\partial x_i} + \frac{\partial\bar{\tau}_{ij}}{\partial x_j} \quad (2)$$

Where x_i and \bar{u}_i are the position and velocity vector, ρ is the fluid density, $\overline{\rho u'_i u'_j}$ is the Reynolds stress tensor, \bar{p} is the mean pressure, t is the time and $\bar{\tau}_{ij}$ is the mean viscous stress tensor $\bar{\tau}_{ij}$ is defined as follows:

$$\bar{\tau}_{ij} = \mu \left(\frac{\partial\bar{u}_i}{\partial x_j} + \frac{\partial\bar{u}_j}{\partial x_i} \right) \quad (3)$$

Where μ is the dynamic viscosity.

2.2 Turbulence Models

Realizable k- ϵ two layer, which is model that solves equations for turbulence kinetic energy (k) and the turbulence dissipation rate (ϵ) in order to determine the eddy viscosity μ_t by equation:

$$\mu_t = \rho C_\mu f_\mu kT \quad (4)$$

Where f_μ is a damping function, T is a turbulent time scale and C_μ is a model coefficient. Eq. (5) determines the turbulent time scale as follows:

$$T = T_e \quad (5)$$

Where $T_e = k / \varepsilon$ is the large-eddy time scale. The transport equations for k and the ε are given as follows:

$$\frac{\partial}{\partial t}(\rho k) + \nabla \cdot (\rho k \bar{v}) = \nabla \cdot \left[\left(\mu + \frac{\mu_t}{\sigma_k} \right) \nabla k \right] + P_k - \rho(\varepsilon - \varepsilon_0) + S_k \quad (6)$$

$$\frac{\partial}{\partial t}(\rho \varepsilon) + \nabla \cdot (\rho \varepsilon \bar{v}) = \nabla \cdot \left[\left(\mu + \frac{\mu_t}{\sigma_\varepsilon} \right) \nabla \varepsilon \right] + \frac{1}{T_e} C_{\varepsilon 1} P_\varepsilon - C_{\varepsilon 2} f_{2\rho} \left(\frac{\varepsilon}{T_e} - \frac{\varepsilon_0}{T_0} \right) + S_\varepsilon \quad (7)$$

Production terms P_k and P_ε are given by Eq. (8) as follows:

$$P_k = f_c G_k + G_b - \gamma_M; \quad P_\varepsilon = f_c S k + C_{\varepsilon 3} G_b \quad (8)$$

The damping functions is given by Eq. (9) as follow:

$$f_2 = \frac{k}{k + \sqrt{\nu \varepsilon}}; \quad f_\mu = \frac{1}{C_\mu \left\{ 4 + \sqrt{6} \cos \left[\frac{1}{3} \cos^{-1} \left(\sqrt{6} \frac{S^{*3}}{\sqrt{S^* : S^*}^3} \right) \right] \right\}} \frac{k}{\varepsilon} \sqrt{S : S + W : W} \quad (9)$$

3. Numerical Simulations

3.1 General Information of a KCS Containership

The research object is a KCS containership. This ship is often applied in studying the flow around the ship by RANSE method as its 3D model and experimental results are published online [27,28]. Table 1 and Figure 1 illustrate the KCS containership at model scales of 1/31.6 and full scale.

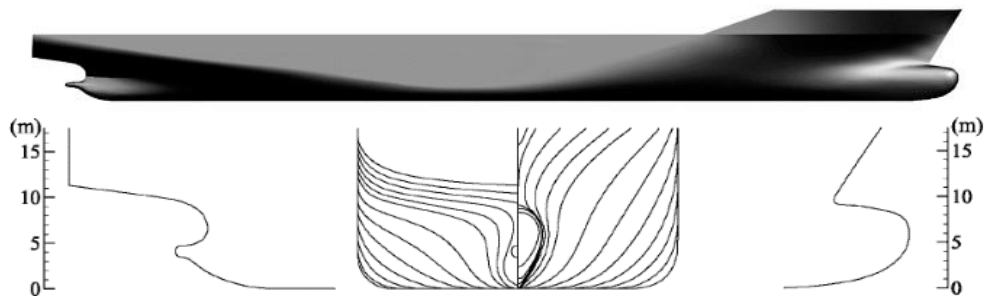


Fig. 1. KCS container ship model

Table 1
 Main characteristics of KCS containership

| Parameters | Symbol | Unit | Value | |
|---------------------|----------|-------------------|------------|-------|
| | | | Full scale | Model |
| Length of the ship | L_{PP} | [m] | 230.00 | 7.278 |
| Breadth of the ship | B | [m] | 32.20 | 1.019 |
| Draught of the ship | T | [m] | 10.80 | 0.341 |
| Displacement | ∇ | [m ³] | 52030 | 1.649 |
| Wetted surface area | S | [m ²] | 9530 | 9.544 |

3.2 Simulation Setup

3.2.1 Computational conditions and case studies

The influence of the model scale on the change of flow characteristics around the ship hull is stimulated with the following computational cases and conditions:

- i. Simulation at two different scales including full scale and ship model with a scale of 1/31.6. These two scales are considered because it is possible to compare the simulation results and the experiment ones in the towing tank and the actual transferred calculation results to the full scale ship, which have been provided in [27,29,30].
- ii. The environmental conditions considered for the ship at the model and full scale are taken the same as the test conditions in [27,29].

3.2.2 Computational domain size and boundary condition

The size of the virtual towing tank was defined as corresponding to the guidelines of the International Towing Tank Conferences [31]. Typically, the domain length is extended $1.5L_{PP}$ forward the ship bow and $2.5L_{PP}$ backward its stern. Meanwhile, the bottom and top of the virtual towing tank are placed at a distance of $2.5L_{PP}$ and $1.5L_{PP}$ from the free surface, respectively. The sidewall of the virtual towing tank is placed at a distance of $2.5L_{PP}$ from the longitudinal symmetric plane of the vessel (see Figure 2).

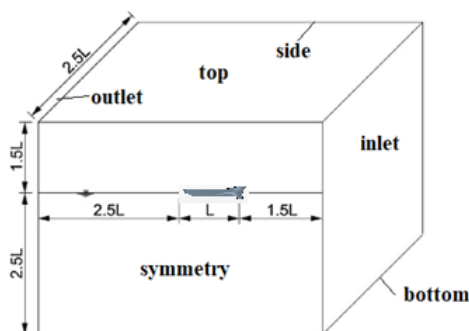


Fig. 2. The size of virtual towing tank

The type of boundary conditions is defined as follows: The velocity inlet is applied on inlet, top and bottom of virtual towing tank, the flow behind the hull is pressure outlet, the two sides of virtual towing tank are the symmetry plane. No-slip wall condition is used on the ship hull [32].

3.2.3 Mesh generation and physical model

Mesh type and mesh generation have a significant effect on the numerical simulation results. In the prediction of ship resistance using RANSE method, 3 types of mesh are used: surface mesh, trimmed mesh, and prism mesh [33]. In order to minimize the number of meshes used while keeping acceptable accuracy of the simulation results, the mesh will be refined in the vicinity of the ship (especially in the bow and stern regions having complex curvature), at the free surface to have the best capture of Kelvin waves.

The mesh generation will be done in the same manner for the ship at model scale and the full-scale ship, the only difference is the wall thickness of the first layer of the prism mesh of the full-scale ship and the model scale to ensure that the average value of Y^+ of the model ship is 50 and the mean value of Y^+ of the full-scale ship is about 400 (see Figure 3). The resulting of mesh generation for the model and the full-scale ship are depicted in Figure 4.

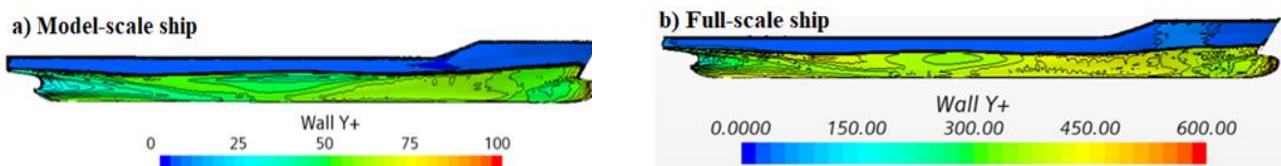


Fig. 3. Y^+ value on hull surface

The physical model used in the ship resistance simulation is a real fluid model (viscous and incompressible) using the Unsteady RANSE. The Realizable $k-\epsilon$ two layer turbulent model is used to close the RANSE equation, as according to [34,35] the Realizable $k-\epsilon$ two layer turbulent model provides relatively accurate results in calculating the ship hydrodynamics in general and ship resistance in particular. The Volume of Fluid method is employed to solve the free surface. The DFBI Equilibrium option is used to model motion of the ship with two degrees of freedom (trim and sinkage).

One of the key issues determining the accuracy of numerical results is choosing the time step. For resistance simulation, according to ITTC procedures [36] the time step is defined by Eq. (10) as follows:

$$\Delta t = 0.005 \square 0.01L / V \quad (10)$$

where L and V are the ship's length and speed, respectively.

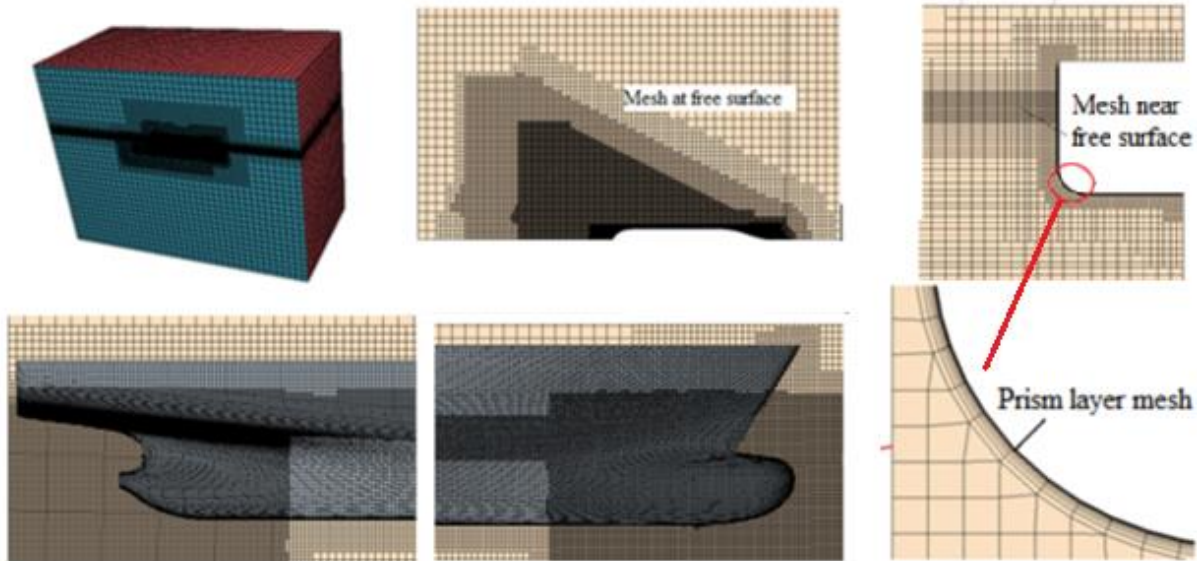


Fig. 4. Structure of mesh

4. Simulation Results

4.1 Mesh Convergence Study

It is crucial to study the convergence of the mesh at the beginning of numerical calculation. Following the Guidelines provided by ITTC [37], in this research, the authors studied the mesh convergence at $Fr=0.260$ with 3 sizes of mesh including coarse, medium, and fine mesh which are generated by the refinement ratio $r_G = \sqrt{2}$. As a result, the numbers of mesh cells used in the simulation for model scale is 0.79, 1.77, and 3.71 million cells, respectively. Meanwhile, those are 1.02, 2.08, 4.79 million cells, respectively at the full-scale simulation. Eq. (11) depicts the definition of convergence ratio:

$$R_G = \varepsilon_{21} / \varepsilon_{32} \quad (11)$$

When $R_G > 1$, the mesh is not converged; and if $R_G < 0$, the mesh is oscillatory convergence. Otherwise, it is known as monotonous convergence. ε_{12} and ε_{23} can be estimated as follows:

$$\varepsilon_{21} = (S_1 - S_2) / S_1; \varepsilon_{32} = (S_2 - S_3) / S_2 \quad (12)$$

Where S_1, S_2, S_3 – are resistance obtained by fine, medium, and coarse meshes, respectively. The results deflection between numerical simulation (S) results and towing tank experiment measurements (D) is estimated as follows:

$$E\%D = \frac{(D - S)}{D} \cdot 100\% \quad (13)$$

Table 2 depicts the mesh convergence results for ship at model and full scale. It can be observed from Table 2 that, the mesh is monotonous convergence as increasing the number of mesh cells. The simulation result obtained by fine mesh is close to the towing tank measurement (for ship at model scale) and the extrapolate result to full-scale ship. In particular, the difference in the ship total resistance coefficient (C_T), between simulation results and experimental measurements, at model

and full scale are 1.08% and 3.22%, respectively. Thus, the fine mesh is selected to visualize the difference of flow around the ship hull at different model scales. Moreover, it can be seen from Table 2 a huge difference in the frictional resistance component (CF) between model and full- scale ships. Specifically, this coefficient is twice times larger in model scale than in full scale ships. This can be explained by the difference in Reynolds number between the model scale and full-scale ships, leading to the difference in the shear stress coefficient on the hull surface shown below this paper.

Table 2
 The mesh convergence results at Fr=0.260

| Parameters | EFD (D) [28] | Mesh | | | ε ₃₂ % | ε ₂₁ % | R _G | |
|--------------------------------------|--------------|--------|--------|-------|-------------------|-------------------|----------------|------|
| | | Coarse | Medium | Fine | | | | |
| Ship at model scale | | | | | | | | |
| C _T x10 ⁻³ [-] | Value | 3.711 | 3.845 | 3.815 | 3.751 | -0.79 | -0.02 | 0.02 |
| | E%D | / | 3.610 | 2.800 | 1.080 | / | / | / |
| C _F x10 ⁻³ [-] | Value | / | 3.341 | 3.328 | 3.311 | -0.39 | -0.01 | 0.01 |
| C _P x10 ⁻³ [-] | Value | / | 0.504 | 0.487 | 0.440 | -3.49 | -0.11 | 0.03 |
| Full scale ship | | | | | | | | |
| C _T x10 ⁻³ [-] | Value | 2.361 | 2.516 | 2.457 | 2.437 | -2.40 | -0.82 | 0.34 |
| | E%D | / | 6.570 | 4.070 | 3.220 | / | / | / |
| C _F x10 ⁻³ [-] | Value | / | 1.591 | 1.586 | 1.583 | -0.32 | -0.19 | 0.60 |
| C _P x10 ⁻³ [-] | Value | / | 0.925 | 0.871 | 0.854 | -6.20 | -1.99 | 0.32 |

4.2 Influence of Model Scale on the Flow Around the Ship

4.2.1 Wave pattern at the free surface and wave profile along ship hull

The influence of scale effect on wave shape at free surface and wave profile along the ship hull at Fr=0.26 is presented in Figures 5 and 6.

It can be observed in those figures, the difference in surface wave shape between the model scale and full-scale ship appears in the wake flow behind the ship hull. Especially, the stern wave created by the moving ship at full-scale ship is bigger than obtained at the model scale. Otherwise, concern to the profile of wave along the ship hull, the discrepancy located near the ship bow and stern. The wave profile obtained at full scale is greater than that of model scale. These results are coincident with the results published by the previous worldwide authors [25].

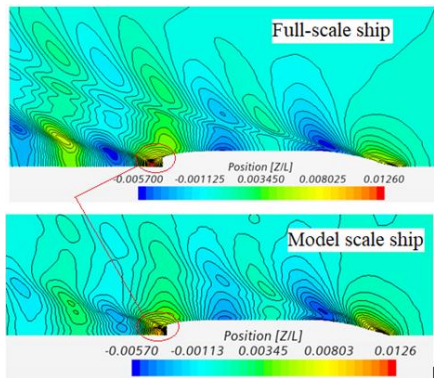


Fig. 5. Influence of model scale on the surface wave shape at Fr=0.260

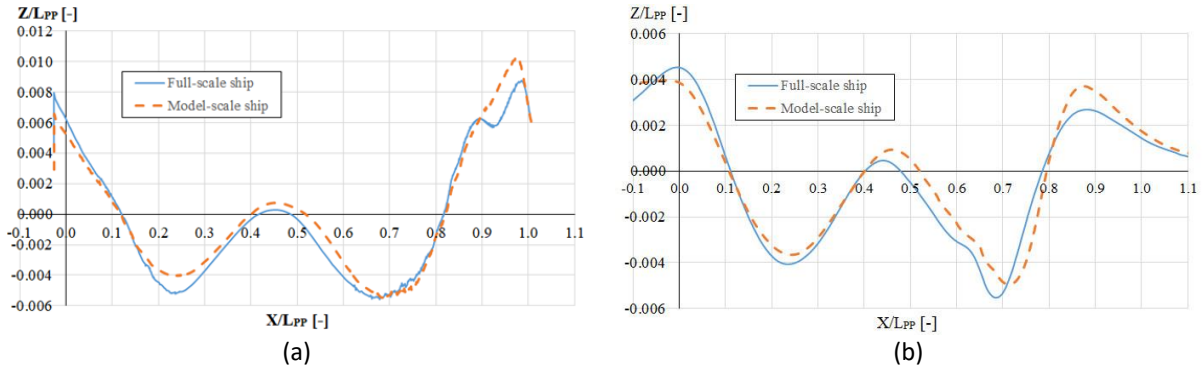


Fig. 6. Comparison of wave profiles between model and full scale (a) along the ship (b) at $y/L_{pp} = 0.1$

4.2.2 Distribution of shear stress coefficient on the model hull

The influences of model scale on the distribution of shear stress on the ship surface at different speeds are depicted in Figures 7, 8 and 9. It can be observed from these figures that the model scale has a great impact on shear stress coefficient on the ship surface. The greater the model scale (the smaller the model), the bigger the shear stress coefficient is and vice versa. That can partly be explained by the difference in Reynolds numbers between each model. This difference also leads to the bigger ship friction resistance at model scale than at the full scale.

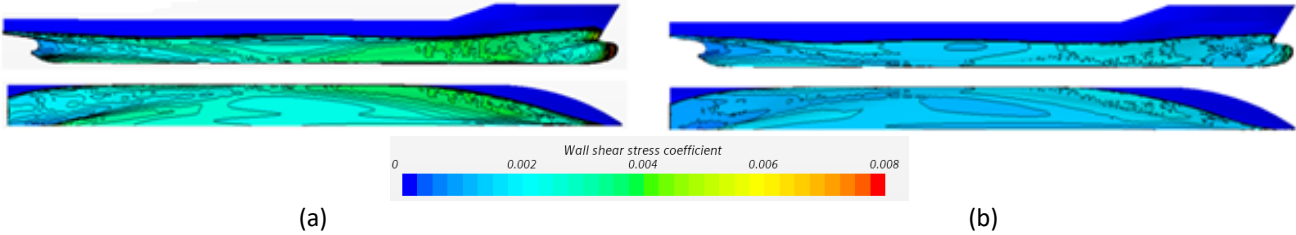


Fig. 7. Influence scale effect on shear stress distribution on the ship surface at $Fr=0.260$ (a) Model scale; (b) Full scale

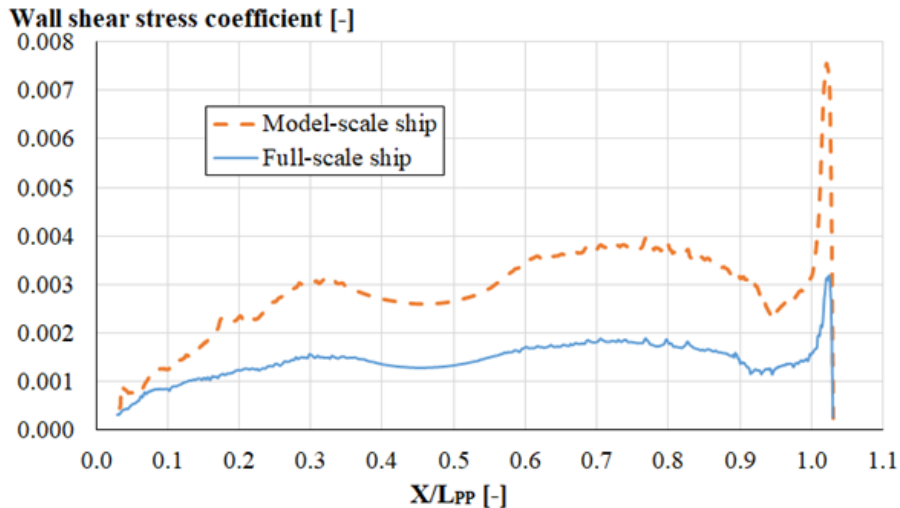


Fig. 8. The influence scale effect on shear stress distribution at $Z/T = 0.5$ and $Fr = 0.260$

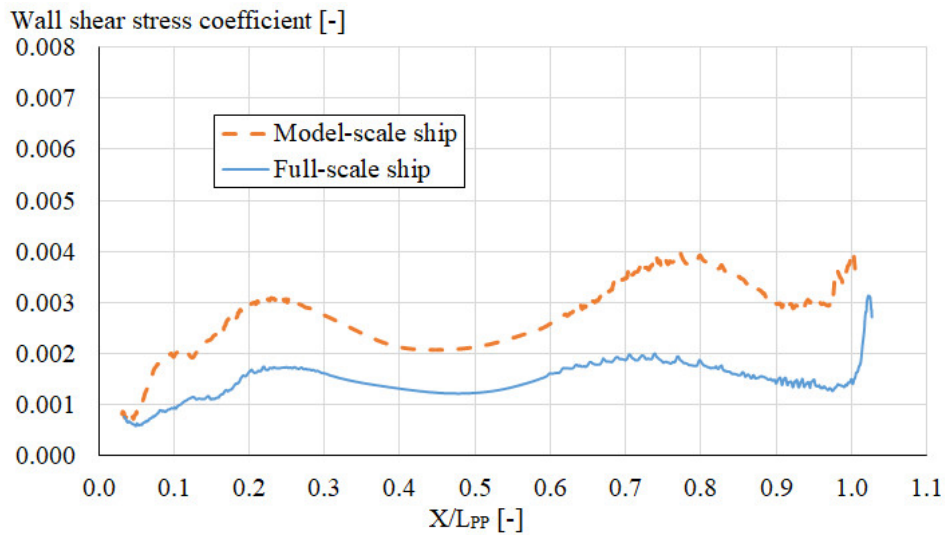


Fig. 9. The influence scale effect on shear stress distribution at $Z/T = 0.25$ and $Fr = 0.260$

4.2.3 Distribution of pressure on the hull surface

Figures 10 and 11 depict the influence of scale effect on the distribution of pressure on the surface of the ship at various speeds. It can be observed from these figures that the model scale has smaller effect on the dynamic pressure distribution than the shear stress distribution. Moreover, the difference in dynamic pressure mainly appears in the vicinity of ship stern and it increases as reducing the scale of the model.

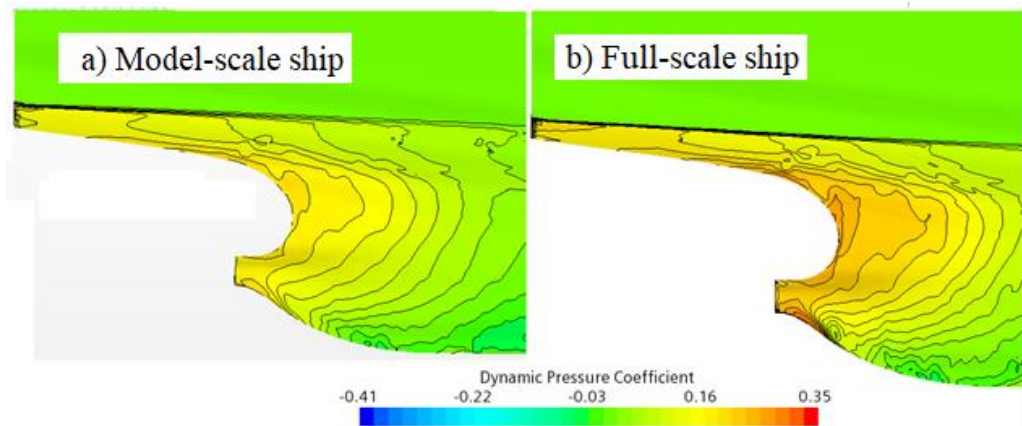


Fig. 10. The influence of model scale on dynamic pressure distributed on the hull surface at $Fr = 0.260$

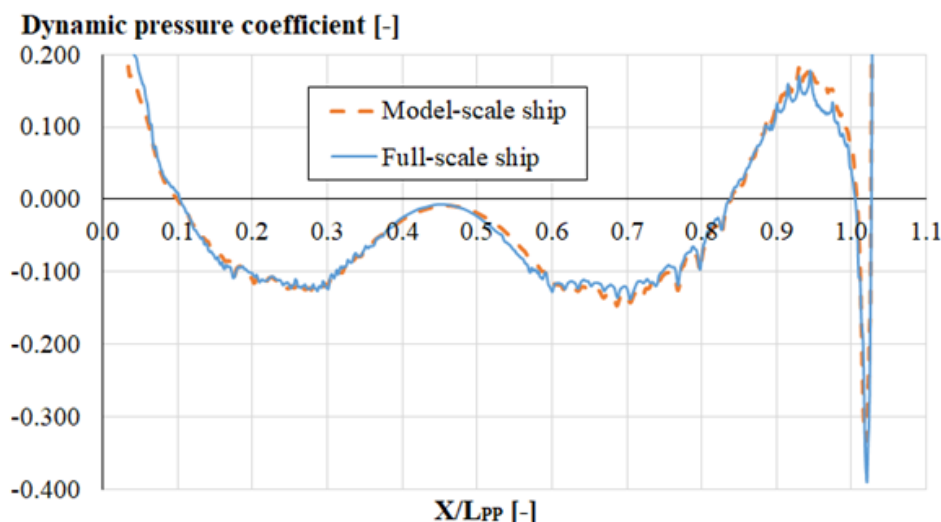


Fig. 11. The influence of model scale on dynamic pressure distribution at $Z/T = 0.5$ and $Fr = 0.260$

4.2.4 Wake field at propeller disc

The influence of the model scale on the wake field behind the ship hull at propeller disc ($x=0.0175L_{PP}$) is presented in Figure 12. It can be observed that, the model scale has a significant impact on the wake field. The greater the model scale (ship model), the larger wake field is as the Reynolds number of the ship model is smaller than that of the full scale.

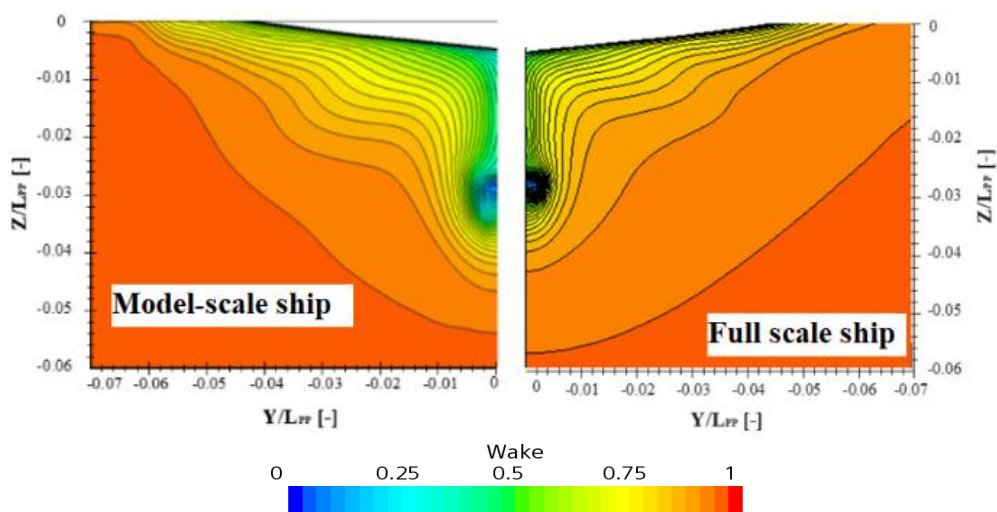


Fig. 12. The influence of model scale on wake field behind the ship hull at propeller disc and $Fr = 0.260$

5. Conclusions

This research has succeeded in using RANSE method to study the influence of model scale on the change of flow field around the ship. The achievements are mentioned as follows:

- i. Predicted the ship resistance at model scale and full scale. The simulation results are close to the measurements obtained in towing tank and the full-scale ship converted according to ITTC's guidelines with differences are 1.08% and 3.22%, respectively.

- ii. Provided and analyzed the influence of model scale on the change of flow around the hull characteristics including surface wave shape created by the ship's movement, wave profile along the ship hull, wake field at the propeller disc. These pieces of information may support the designer in defining the optimal hull form, predicting ship power, and other systems with higher accuracy.

Acknowledgment

We acknowledge the support of time and facilities from Ho Chi Minh City University of Technology (HCMUT), Vietnam National University Ho Chi Minh City (VNU-HCM) for this study.

References

- [1] Dogrul, Ali, Soonseok Song, and Yigit Kemal Demirel. "Scale effect on ship resistance components and form factor." *Ocean Engineering* 209 (2020): 107428. <https://doi.org/10.1016/j.oceaneng.2020.107428>
- [2] Bhushan, Shanti, Tao Xing, Pablo Carrica, and Frederick Stern. "Model-and full-scale URANS simulations of Athena resistance, powering, seakeeping, and 5415 maneuvering." *Journal of Ship Research* 53, no. 04 (2009): 179-198. <https://doi.org/10.5957/jsr.2009.53.4.179>
- [3] Terziev, Momchil, Tahsin Tezdogan, and Atila Incecik. "Scale effects and full-scale ship hydrodynamics: A review." *Ocean Engineering* 245 (2022): 110496. <https://doi.org/10.1016/j.oceaneng.2021.110496>
- [4] Song, Ke-wei, Chun-yu Guo, Chao Wang, Cong Sun, Ping Li, and Ruo-fan Zhong. "Experimental and numerical study on the scale effect of stern flap on ship resistance and flow field." *Ships and Offshore Structures* 15, no. 9 (2020): 981-997. <https://doi.org/10.1080/17445302.2019.1697091>
- [5] Abobaker, Mostafa, Sogair Addeep, Lukmon O. Afolabi, and Abdulhafid M. Elfaghi. "Effect of Mesh Type on Numerical Computation of Aerodynamic Coefficients of NACA 0012 Airfoil." *Journal of Advanced Research in Fluid Mechanics and Thermal Sciences* 87, no. 3 (2021): 31-39. <https://doi.org/10.37934/arfmts.87.3.3139>
- [6] Arafat, Mohammad, Izuan Amin Ishak, Ahmad Faiz Mohammad, Amir Khalid, Md Norrizam Mohmad Jaát, and Mohd Fuad Yasak. "Effect of Reynolds number on the wake of a Next-Generation High-Speed Train using CFD analysis." *CFD Letters* 15, no. 1 (2023): 76-87. <https://doi.org/10.37934/cfdl.15.1.7687>
- [7] Subramaniam, Thineshwaran, and Mohammad Rasidi Rasani. "Pulsatile CFD Numerical Simulation to investigate the effect of various degree and position of stenosis on carotid artery hemodynamics." *Journal of Advanced Research in Applied Sciences and Engineering Technology* 26, no. 2 (2022): 29-40. <https://doi.org/10.37934/araset.26.2.2940>
- [8] Le, Tat-Hien, Mai The Vu, Vu Ngoc Bich, Nguyen Kim Phuong, Nguyen Thi Hai Ha, Tran Quoc Chuan, and Tran Ngoc Tu. "Numerical investigation on the effect of trim on ship resistance by RANSE method." *Applied Ocean Research* 111 (2021): 102642. <https://doi.org/10.1016/j.apor.2021.102642>
- [9] Hoa, Nguyen Thi Ngoc, Bich Ngoc Vu, Ngoc Tu Tran, Nguyen Manh Chien, and Tat Hien Le. "Numerical investigating the effect of water depth on ship resistance using RANS CFD method." *Polish Maritime Research* (2019). <https://doi.org/10.2478/pomr-2019-0046>
- [10] Tu, Tran Ngoc, Do Duc Luu, Nguyen Thi Hai Ha, Nguyen Thi Thu Quynh, and Nguyen Minh Vu. "Numerical prediction of propeller-hull interaction characteristics using RANS method." *Polish Maritime Research* 2 (2019): 163-172. <https://doi.org/10.2478/pomr-2019-0036>
- [11] Tu, Tran Ngoc. "Numerical simulation of propeller open water characteristics using RANSE method." *Alexandria Engineering Journal* 58, no. 2 (2019): 531-537. <https://doi.org/10.1016/j.aej.2019.05.005>
- [12] Niklas, Karol, and Hanna Prusko. "Full-scale CFD simulations for the determination of ship resistance as a rational, alternative method to towing tank experiments." *Ocean Engineering* 190 (2019): 106435. <https://doi.org/10.1016/j.aej.2019.05.005>
- [13] Can, Ugur, Cihad Delen, and Sakir Bal. "Effective wake estimation of KCS hull at full-scale by GEOSIM method based on CFD." *Ocean Engineering* 218 (2020): 108052. <https://doi.org/10.1016/j.oceaneng.2020.108052>
- [14] Luu, Do Duc, Tran Ngoc Tu, Tran Khanh Toan, Tat-Hien Le, Nguyen Duy Anh, and Nguyen Thi Hai Ha. "Numerical Study on the Influence of Longitudinal Position of Centre of Buoyancy on Ship Resistance Using RANSE Method." *Naval Engineers Journal* 132, no. 4 (2020): 151-160.
- [15] Kraskowski, Marek. "CFD Optimisation of the Longitudinal Volume Distribution of a Ship's Hull by Constrained Transformation of the Sectional Area Curve." *Polish Maritime Research* 29, no. 3 (2022): 11-20. <https://doi.org/10.2478/pomr-2022-0022>

- [16] Saydam, Ahmet Ziya, Serhan Gokcay, and Mustafa Insel. "CFD based vortex generator design and full-scale testing for wake non-uniformity reduction." *Ocean Engineering* 153 (2018): 282-296. <https://doi.org/10.1016/j.oceaneng.2018.01.097>
- [17] Jasak, Hrvoje, Vuko Vukčević, Inno Gatin, and Igor Lalović. "CFD validation and grid sensitivity studies of full scale ship self propulsion." *International Journal of Naval Architecture and Ocean Engineering* 11, no. 1 (2019): 33-43. <https://doi.org/10.1016/j.ijnaoe.2017.12.004>
- [18] Choi, J. E., K-S. Min, J. H. Kim, S. B. Lee, and H. W. Seo. "Resistance and propulsion characteristics of various commercial ships based on CFD results." *Ocean engineering* 37, no. 7 (2010): 549-566. <https://doi.org/10.1016/j.oceaneng.2010.02.007>
- [19] Farkas, Andrea, Soonseok Song, Nastia Degiuli, Ivana Martić, and Yigit Kemal Demirel. "Impact of biofilm on the ship propulsion characteristics and the speed reduction." *Ocean Engineering* 199 (2020): 107033. <https://doi.org/10.1016/j.oceaneng.2020.107033>
- [20] Sun, Wenyu, Qiong Hu, Shiliang Hu, Jia Su, Jie Xu, Jinfang Wei, and Guofu Huang. "Numerical analysis of full-scale ship self-propulsion performance with direct comparison to statistical sea trial results." *Journal of marine science and engineering* 8, no. 1 (2020): 24. <https://doi.org/10.3390/jmse8010024>
- [21] Tran, Thai Gia, and CV HUYNH. "Improving the accuracy of ship resistance prediction using computational fluid dynamics tool." *International Journal on Advanced Science Engineering Information Technology* 10, no. 1 (2020): 171-177. <https://doi.org/10.18517/ijaseit.10.1.10588>
- [22] Nabawi, Rahmat Azis. "Study Reduction of Resistance on The Flat Hull Ship of The Semi-Trimaran Model: Hull Vane Vs Stern Foil." *CFD Letters* 13, no. 12 (2021): 32-44. <https://doi.org/10.37934/cfdl.13.12.3244>
- [23] Nasirudin, Ahmad, I. Ketut Aria Pria Utama, and Andreas Kukuh Priyasambada. "CFD Analysis into the Resistance Estimation of Hard-Chine Monohull using Conventional against Inverted Bows." *CFD Letters* 15, no. 6 (2023): 54-64. <https://doi.org/10.37934/cfdl.15.6.5464>
- [24] Tu, Tran Ngoc, Marek Kraskowski, Nguyen Manh Chien, Vu Tuan Anh, Do Luc Luu, and Nguyen Kim Phuong. "Numerical study on the influence of trim on ship resistance in trim optimization process." *Naval Engineers Journal* 130, no. 4 (2018): 133-142.
- [25] Hänninen, Satu, and Juha Sehweighofer. "Numerical investigation of the scale effect on the flow around a ship hull." *Ship Technology Research* 53, no. 1 (2006): 17-25. <https://doi.org/10.1179/str.2006.53.1.004>
- [26] Hochkirch, Karsten, and Benoit Mallol. "On the importance of full-scale CFD simulations for ships." In *11th International conference on computer and IT applications in the maritime industries, COMPIT*. 2013.
- [27] *SIMMAN 2008 Workshop*, [Online]. Available from: <http://www.simman2008.dk/kcs/container.html>.
- [28] Hino, Takanori, Frederick Stern, Lars Larsson, Michel Visonneau, Nobuyuki Hirata, and Jin Kim, eds. *Numerical ship hydrodynamics: an assessment of the Tokyo 2015 Workshop*. Vol. 94. Springer Nature, 2020. <https://doi.org/10.1179/str.2006.53.1.004>
- [29] Kim, W. J., S. H. Van, and D. H. Kim. "Measurement of flows around modern commercial ship models." *Experiments in fluids* 31, no. 5 (2001): 567-578. <https://doi.org/10.1007/s003480100332>
- [30] Technical report results of resistance test for containership KCS. CTO, Poland 2017.
- [31] *ITTC 2014. Recommended procedures and guidelines 7.5-03-02-04*. Available from: <https://itc.info/media/4198/75-03-02-04.pdf>.
- [32] Tu, Tran Ngoc, Do Duc Luu, Nguyen Thi Hai Ha, Nguyen Thi Thu Quynh, and Nguyen Minh Vu. "Numerical prediction of propeller-hull interaction characteristics using RANS method." *Polish Maritime Research* 2 (2019): 163-172. <https://doi.org/10.2478/pomr-2019-0036>
- [33] Choi, J. E., K-S. Min, J. H. Kim, S. B. Lee, and H. W. Seo. "Resistance and propulsion characteristics of various commercial ships based on CFD results." *Ocean engineering* 37, no. 7 (2010): 549-566. <https://doi.org/10.1016/j.oceaneng.2010.02.007>
- [34] Yong, Zhao, Zong Zhi, Zou Li, and Wang Tianlin. "Turbulence model investigations on the boundary layer flow with adverse pressure gradients." *Journal of Marine Science and Application* 14, no. 2 (2015): 170-174. <https://doi.org/10.1007/s11804-015-1303-0>
- [35] Tu, Tran Ngoc, Vu Minh Ngoc, Nguyen Thi Thu Quynh, Nguyen Manh Chien, Nguyen Thi Hai Ha, and Nguyen Thi Ha Phuong. "Effects of Turbulence Models On RANSE Computation Of Flow Around DTMB 5415 Vessel." *Naval Engineers Journal* 133, no. 3 (2021): 137-151.
- [36] Procedures, ITTC Recommended. "Uncertainty analysis in CFD verification and validation, methodology and procedures." *ITTC Recommended Procedures and Guidelines* (2017): 7-5.
- [37] ITTC Specialist Committee. "Recommended procedures and guidelines-uncertainty analysis in CFD verification and validation methodology and procedures." In *28th International Towing Tank Conference*. 2017.